Hindawi Publishing Corporation
International Journal of Photoenergy
Volume 2014, Article ID 291904, 8 pages
http://dx.doi.org/10.1155/2014/291904

Research Article

Performance Improvements of Selective Emitters by Laser Openings on Large-Area Multicrystalline Si Solar Cells

Sheng-Shih Wang,[1] Jyh-Jier Ho,[1] Jia-Jhe Liou,[1] Jia-Show Ho,[2] Wei-Chih Hsu,[3] Wen-Haw Lu,[3] Song-Yeu Tsai,[3] Hsien-Seng Hung,[1] and Kang L. Wang[2]

[1] *Department of Electrical Engineering, National Taiwan Ocean University, No. 2 Peining Road, Keelung 20224, Taiwan*
[2] *Department of Electrical Engineering, University of California, Los Angeles, CA 90095, USA*
[3] *Laboratory of Green Energy & Environment Research, Industrial Technology Research Institute, No. 195 Chung-Hsing Road, Section 4, Chutung, Hsinchu 31061, Taiwan*

Correspondence should be addressed to Jyh-Jier Ho; jackho@mail.ntou.edu.tw

Received 10 November 2013; Accepted 24 March 2014; Published 17 April 2014

Academic Editor: Mohammed A. Gondal

This study focuses on the laser opening technique used to form a selective emitter (SE) structure on multicrystalline silicon (mc-Si). This technique can be used in the large-area ($156 \times 156\ mm^2$) solar cells. SE process of this investigation was performed using 3 samples SE1–SE3. Laser fluences can vary in range of 2–5 J/cm^2. The optimal conversion efficiency of 15.95% is obtained with the SE3 (2 J/cm^2 fluence) after laser opening with optimization of heavy and light dopant, which yields a gain of $0.48\%_{abs}$ compared with that of a reference cell (without fluence). In addition, this optimal SE3 cell displays improved characteristics compared with other cells with a higher average value of external quantum efficiency ($EQE_{avg} = 68.6\%$) and a lower average value of power loss ($P_{loss} = 2.33\ mW/cm^2$). For the fabrication of solar cells, the laser opening process comprises fewer steps than traditional photolithography does. Furthermore, the laser opening process decreases consumption of chemical materials; therefore, the laser opening process decreases both time and cost. Therefore, SE process is simple, cheap, and suitable for commercialization. Moreover, the prominent features of the process render it effective means to promote overall performance in the photovoltaic industry.

1. Introduction

Because of the simple manufacturing process and low-cost crystalline-silicon (C-Si) material, multicrystalline Si (mc-Si) solar cells are more widely used than single-crystalline Si (sc-Si) solar cells in the commercial market. In general, homogenous emitters (HEs) for effective photovoltaic (PV) devices are formed on the front surface through high phosphorus concentration. This is necessary because a strong metal contact reduces the resistance between a metal grid and a silicon wafer. However, this process also leads to severe recombination on the front side, also called a dead layer, greatly reducing the solar-cell performance [1]. To optimize the emitter layer, an SE structure is proposed in this study to overcome this compromise. This reduces the contact resistance and surface recombination velocity and improves the performance of cells [2–5].

For the applications of large-area SE solar cells in the PV industry, intensive research has been conducted, using back etching [2], paste etching [3], laser doping [4], and two-diffusion masking [5]. The etchback process, based on the selective etching of the HE that is formed through $POCl_3$ diffusion, uses the metallization approach to create an SE. This SE is obtained in etchback nonprotected regions by using an acidic etch with a bath of HF/HNO_3 until it reaches the appropriate sheet resistance. The disadvantage of the etchback method is that the composition of etching solution is difficult to control accurately, thus lowering its reproducibility. The etching paste technique provides a fast, simple, and reliable method for producing a structure of diffusion barrier layers, which is also of low cost. Nevertheless, certain faults remain, such as a dilation of line width in the opening region. This leads to a much heavier doping region

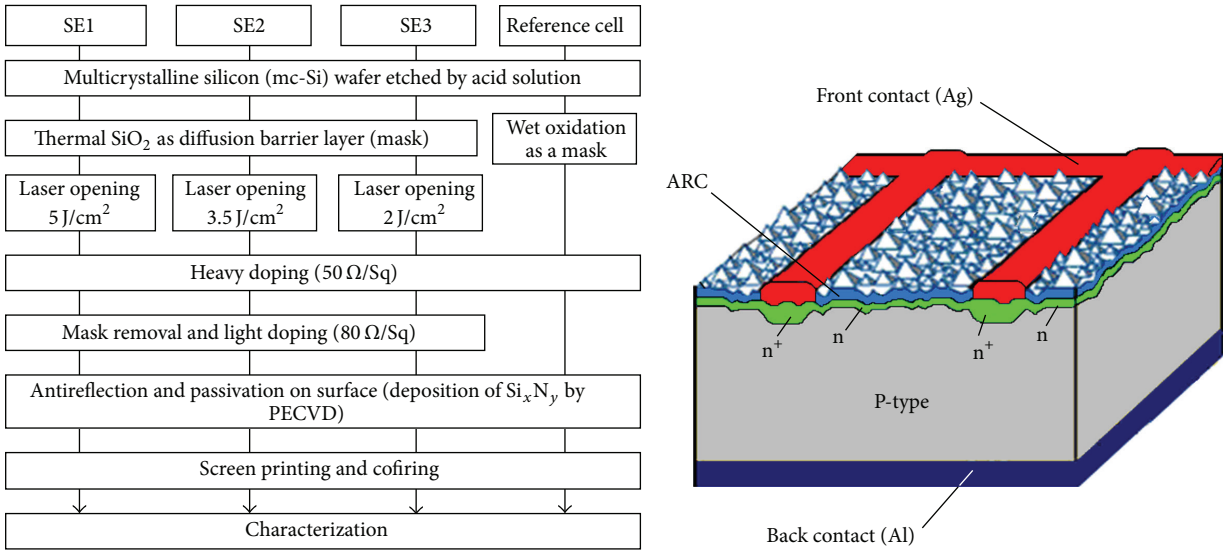

FIGURE 1: (a) Major processing sequence of SE solar cells utilized by laser opening technique. (b) The sketch of our developed solar cell structure.

and a reduction of cell efficiency. Laser doping selectively varies the doping profile on a substrate. Prior to the laser treatment, a doping source is applied to the substrate. The laser locally melts the substrate and diffusion occurs in liquid phase, which is up to 10 orders of magnitude faster than that in solid-state diffusion, thus enabling deep junctions. In addition, the laser selectively melts the Si and locally increases the amount of phosphorous in the emitter. The phosphorus is then driven deeper into the wafer, lowering the sheet resistance of the emitter underneath the metal contact. However, the laser doping process can result in damage that reduces open-circuit voltage (V_{OC}) and filled factor (FF). For the two-diffusion masking technique, an efficiency of 16% is the optimal result for cells realized using the two-diffusion SE process and etching paste ablation. Nevertheless, this technology is relatively complex and the industrialization of this process requires UV laser equipment of high throughput and power; therefore, the production cost of two-diffusion SE cells must be considered.

Laser processing [6], proving suitable for large-area solar cells, has the advantage of highly localized steps and meets the requirements of SE formation. An SE mc-Si solar cell is proposed in this study to overcome the drawbacks of the four aforementioned methods by means of the laser opening process avoiding the photolithography step [7]. In order to improve the performance of the proposed SE mc-Si solar cell, various laser fluences were investigated in the laser opening process. This novel process offers several benefits, including versatility, simplicity, and reliability. Moreover, this cost-effective laser process can be incorporated completely into large-area and high-volume commercial production. In fabricating an SE structure in this study, the two-step $POCl_3$ diffusion processes are also demonstrated. The heavily doped region (HDR) was formed by diffusing through opening areas to reduce contact resistance between the emitter and front side metallization. Subsequently, the lightly doped region (LDR) was used to improve the passivation effect between the contact fingers to increase the PV efficiency for industrial applications.

2. Experimental Procedure

For the fabrication of SE mc-Si solar cells as described previously [7, 8], an Nd:YAG laser (λ = 532 nm and average power (P_{avg}) $\geqq$ 3 W) with a pulse duration of 10–25 ns (@25 kHz) melts the wafer surface. In the first fabrication step of Figure 1(a), texturization of the mc-Si is produced using an acid solution (a mixture of HNO_3 and HF). A silicon dioxide (SiO_2, approximately 10 nm in thickness) is grown through oxidation as the diffusion barrier layer. The procedures of mc-Si texturization and the growth of the diffusion barrier layer are described in a previous study [7]. Laser ablations (at a frequency of 25 kHz, a pulse duration of 10 ns, and under stage speed of 400 mm/s) were next used to open a region in the barrier layer, which acts as a mask, taking advantage of avoiding the photolithography step. Figure 1(a) shows the fabrication procedure of three samples, each with different laser fluences: power levels of 5 J/cm^2 (SE1), 3.5 J/cm^2 (SE2), and 2 J/cm^2 (SE3) and a reference cell (Ref. cell) without SE for comparison.

The SE formed using laser openings has an HDR (50 Ω/sq) under the contact metal with interdigitated fingers followed by deeper $POCl_3$ diffusion. The SiO_2 barrier was removed by an HF-dip to form the second phosphorus diffusion with an LDR (80 Ω/sq) as a shallow emitter. The two-step $POCl_3$ diffusion processes were executed to fine-tune the sheet resistance of heavy/light doping on the developed SE mc-Si solar cells. The Ref. cell was doped homogeneously by using the one-step $POCl_3$ with a sheet resistance of 50 Ω/sq.

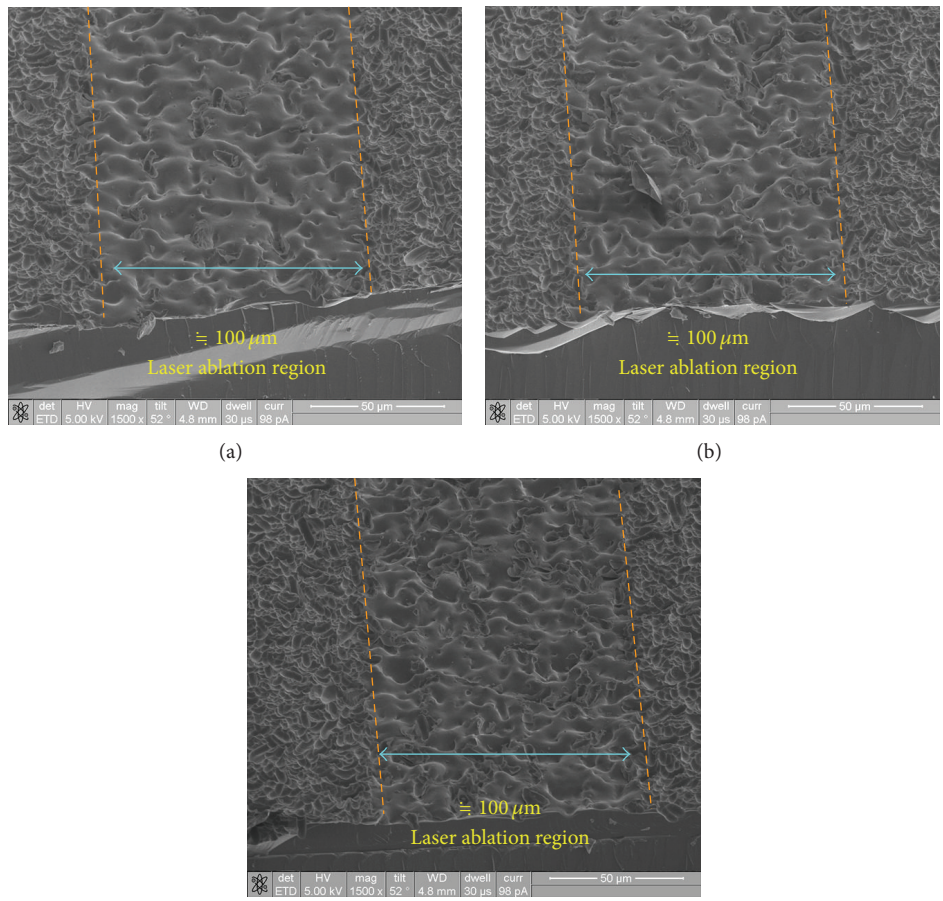

(a) (b) (c)

Figure 2: SEM images of mc-Si wafer after laser ablation process, with the fluences of (a) 5 J/cm^2, (b) 3.5 J/cm^2, and (c) 2 J/cm^2.

The antireflection (AR) and passivation were formed using plasma enhanced chemical vapor deposition (PECVD) Si_xN_y (with 90 nm thickness and 2.1 refractive index) on the front surface. Screen-printing was applied to the solar cells to form metallic contacts. Finally, a laser edge isolation was used to avoid shutting at the front and rear sides. The Ref. cell (50 Ω/sq) with homogeneous doping in the emitter region and without SE was also fabricated for comparison purposes. The experiment results show the laser opening effect on the SE solar-cell application. Figure 1(b) shows the schematic structure of the solar cells investigated in this study. The emitter (green) is lightly doped in shallows and is heavily doped in grooves formed by the laser opening. The cell has 100 nm of Si_xN_y (light blue) by PECVD that acts as an AR layer and a passivating layer. Screen-printing was applied to the solar cell to form an Ag finger on the front side (red region of Figure 1(b)) and an Al surface on the backside (dark-blue region of Figure 1(b)), both as a metallic contact. Therefore, this experiment was primarily focused on using the various laser fluences to optimize the conversion efficiency and lifetime of the solar-cell characteristics. To investigate the characteristics of the laser opening process for SE mc-Si, the performance measurements for the developed solar cells in processing were recorded using a solar simulator (Wacom, WXS-220S-L2) at an air mass of AM 1.5 and illuminated at 1000 W/m^2 by an induced current density-voltage (J-V) tester (Keithley, 4200). The other equipment used comprised a microwave-induced photoconductance decay (μ-PCD) system (Semilab, WT-2000) used to measure lifetime and an incident-photon-to-current-efficiency (IPCE) system (PV Measurements, QEX7) used to measure external quantum efficiency (EQE).

3. Results and Discussions

Figures 2(a)–2(c) show scanning electron microscopy (SEM) images with laser fluences of 5, 3.5, and 2 J/cm^2. The laser-opening process must be conducted by carefully controlling the laser scanning parameters to maintain the metallic contact lines within a width of approximately 100 μm. A distinct surface morphology is evident within the region of laser ablation. The diffusion barrier absorbs the heat and irradiation emitted by the laser for approximately 10 ns. The temperature then quickly increases to melting point (approximately 1417°C). The ablated SiO_2 diffusion barrier layer cools down soon after the irradiation terminates and forms a large, irregular grain in the preselected region for heavy doping.

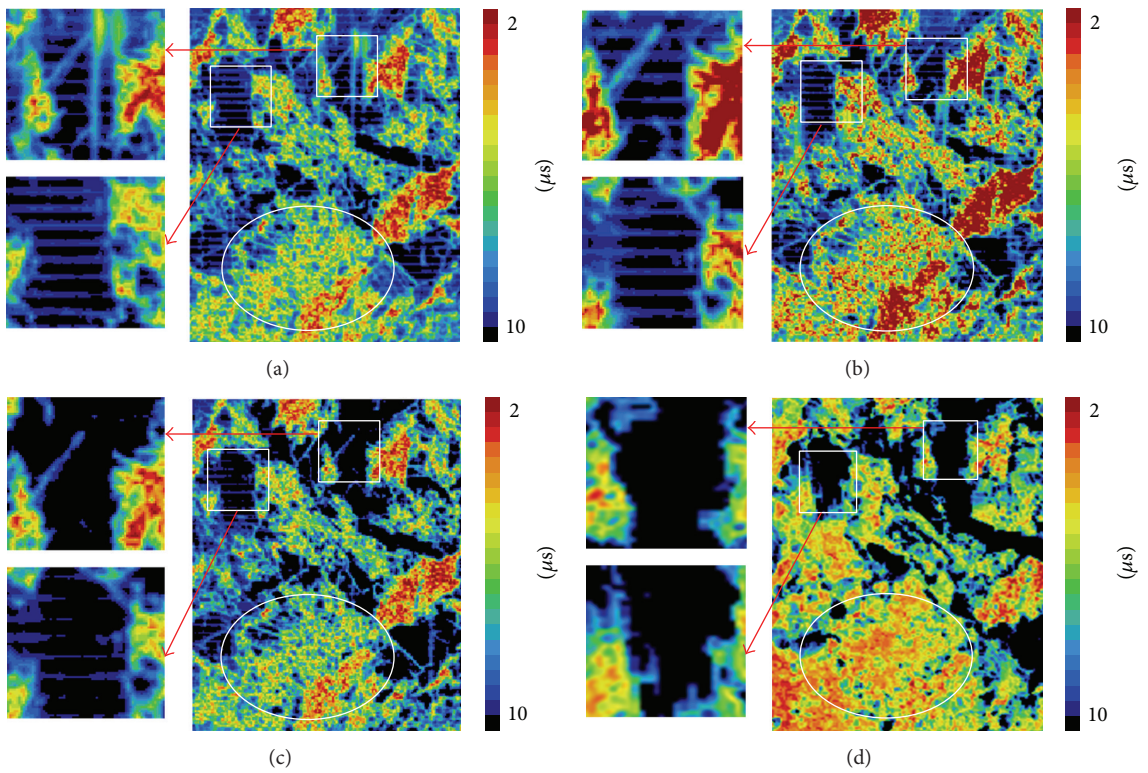

Figure 3: Lifetime mapping of mc-Si wafer after PECVD silicon nitride (Si_xN_y), with laser opening power of (a) 5 J/cm^2 (τ_a = 6.356 μs), (b) 3.5 J/cm^2 (τ_b = 7.162 μs), (c) 2 J/cm^2 (τ_c = 8.082 μs), and (d) reference cell (τ_d = 8.012 μs) without selective emitter (SE).

Table 1: The variation of the average lifetimes (τ, in μs) of mc-Si wafer corresponds to different processes for laser fluences (J/cm^2) of 5, 3.5, 2, and 0 (as a Ref. cell) after steps of acid etching, laser ablation, ARC, and passivation. The average lifetimes for the acid etching step of all samples are 7.36 μs.

After steps of	SE1 (5 J/cm^2)	SE2 (3.5 J/cm^2)	SE3 (2 J/cm^2)	Reference cell
Acid etching	7.36	7.36	7.36	7.36
Laser ablation	4.584	5.574	6.097	—
ARC and passivation	6.356	7.162	8.082	8.012

To investigate the influence of different laser fluences on SE mc-Si solar cells, the frequency and pulse duration of the laser constant were maintained. The surface damage was analyzed by observing the images under an optical μ-PCD microscope. Figures 3(a)–3(c) show lifetime mapping images of mc-Si wafers (SE1, SE2, and SE3) after laser opening with the different laser fluences, followed by depositing an AR passivation layer on both sides. Figure 3(d) is a lifetime mapping image of the Ref. cell. In these μ-PCD images, the dark black-blue regions relate to a low carrier recombination, which indicates an increase in the lifetime of minority charge carriers and further induces currents. However, the light yellow-brown regions correspond to a high carrier recombination, which indicates a decrease in the lifetime and denotes the damage zones.

The short lifetime (τ) measured using laser fluences of 5 J/cm^2 (τ_a = 6.356 μs in Figure 3(a)) and 3.5 J/cm^2 (τ_b = 7.162 μs in Figure 3(b)) indicates the high recombination rate of free carriers in the laser-ablation opening regions. The short lifetime can result from excessive damage induced by a higher laser fluence power. Furthermore, the longest carrier lifetime (τ_c = 8.082 μs in Figure 3(c)) occurs at a laser fluence of 2 J/cm^2 which displays more dark black-blue regions in specific areas. This occurrence is displayed on the left side of the mapping image. This is consistent with the authors' previous study [9], in which reducing the damage region exerted a positive effect on the induced photocurrent while improving the PV device performance.

Table 1 presents the average lifetimes of four cells at different steps in Figure 1(a) where SE1, SE2, and SE3 are laser openings with fluences (J/cm^2) of 5, 3.5, and 2, respectively, and Ref. cell has a fluence of 0. The lifetimes (in μs) were measured after acid etching, laser ablation, ARC, and passivation (deposited Si_xN_y by PECVD).

In this study, the SiO_2 layer, acting as a diffusion barrier, was used to improve the surface passivation properties and

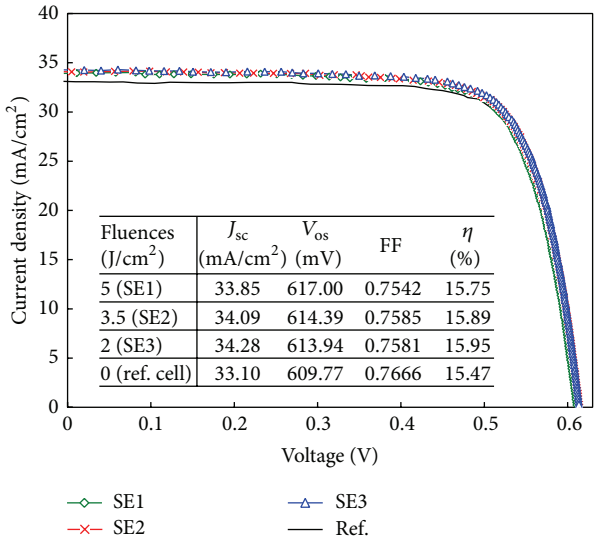

Fluences (J/cm^2)	J_{sc} (mA/cm^2)	V_{os} (mV)	FF	η (%)
5 (SE1)	33.85	617.00	0.7542	15.75
3.5 (SE2)	34.09	614.39	0.7585	15.89
2 (SE3)	34.28	613.94	0.7581	15.95
0 (ref. cell)	33.10	609.77	0.7666	15.47

FIGURE 4: Comparison of current density-voltage (J-V) curves of SE mc-Si solar cells with different laser fluences (5, 3.5, 2, and 0 J/cm^2 for SE1, SE2, SE3, and Ref. cell, resp.) under standard measuring conditions (AM 1.5 spectra, 1000 Wm^{-2}, 25°C). Performances of the developed cells are also included in bottom insert.

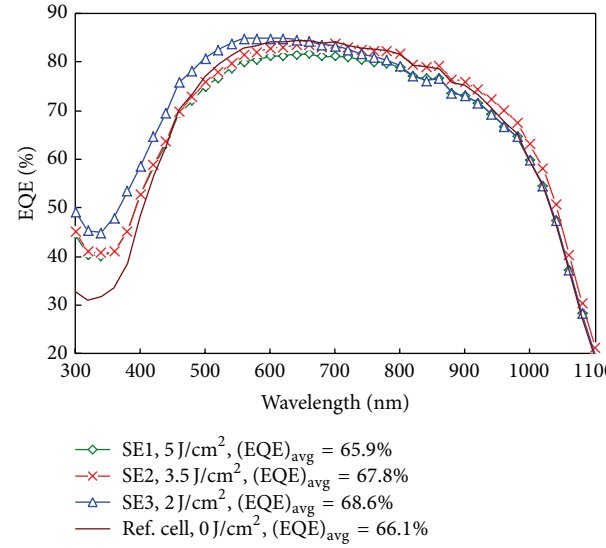

FIGURE 5: Comparison of EQE for SE mc-Si solar cells SE1–SE3 with different laser fluences and Ref. cell without laser fluence.

to clean wafers. However, the low values of the average lifetime (7.36 μs) for acid etching steps of all the samples are not satisfactory for industrial applications. Thus, the wet oxidation process improves the average lifetime of mc-Si wafers because of the reduction of interface defect density by means of passivating surface defects [10]. To improve the performance of the proposed SE mc-Si solar cell, the laser opening process that does not need mask substitutes the wet oxidation. After the laser opening and heavy doping, the average lifetime of the three samples, SE1, SE2, and SE3, increased significantly with the laser fluence decreasing from 5 to 2 J/cm^2. The peak and width of the Gaussian beam rely heavily on laser fluence; a higher laser fluence can create a deeper groove and a larger diameter in opening regions [11, 12]. This generates more damage and thus decreases the lifetime. Accordingly, the average lifetime of mc-Si wafers after laser ablation at a laser fluence of 2 J/cm^2 (6.097 μs) was longer than that at 5 J/cm^2 and 3.5 J/cm^2 (4.584 μs and 5.574 μs, resp.) as shown in Table 1. From the color variation in Figure 3, the laser-opening step caused a significant change in the average lifetime for three different laser fluences, compared with Ref. cell.

An increase in the average lifetime of cells enhances the electrical performance if there is no loss from the laser ablation approach. This is verified by the J-V measurement of the developed cells, as shown in Figure 4. The performance of the SE3 mc-Si solar cell demonstrates the highest short-circuit current density (J_{sc} = 34.28 mA/cm^2) and conversion efficiency (η = 15.95%) and yields a gain of 0.48%$_{abs}$ compared with the Ref cell. From the results of Figure 4, it is clear that the key function of the SE is to improve the value of J_{sc}. The improvement for SE mc-Si solar cells shows a significant increase of the J_{sc} by approximately 2.2%–3.5%, compared with the Ref. cell.

Surface recombination has been identified as a major limiting factor to high efficiency in wafer-Si solar cells [13]. The passivation on the surface of SE solar cells reduces recombination losses, which achieves improved conversion efficiency. The higher conversion efficiency results from electronically passivating the surface of Si, leading to reduced recombination losses. This observation coincides with the results of [14] and reflects the increase in the average lifetime of minority carriers, as confirmed in Table 1. The lower FF is caused by minority carriers crowding at the lateral junction [15, 16] and by resistance from light doping [17].

Figure 5 shows the EQE curves of the developed SE mc-Si solar cells with different laser fluences in a wide-wavelength range (300–1100 nm). The light of shorter wavelengths is absorbed on the front side, considerably close to the surface of the cells because of its high absorption coefficient in silicon. This results in its shallow penetration depth. Such a drop of EQE value can arise from laser-induced damage, which generates carrier recombination. In addition, high laser fluence (SE1 and SE2) damage could be induced, which is also an explanation for the drop in high laser fluence [16, 18]. Therefore, the SE3 cell (with the lowest laser fluence of 2 J/cm^2) has the highest EQE with a wavelength range of 300–600 nm, which could contribute to the low power of laser ablation with a low penetration depth. This increases the high light absorption on the developed mc-SE solar cell. Meanwhile, the EQE of SE3 cells decreases in the long wavelength region (700–900 nm) because of a decrease in diffusion lengths of effective minority carriers. In a whole range of wavelengths, the average EQE values are 65.9%, 67.8%, and 68.6% for SE1, SE2, and SE3, respectively. This indicates a clear laser quality improvement and because the area under the curve is a measure for the SE3 cell current,

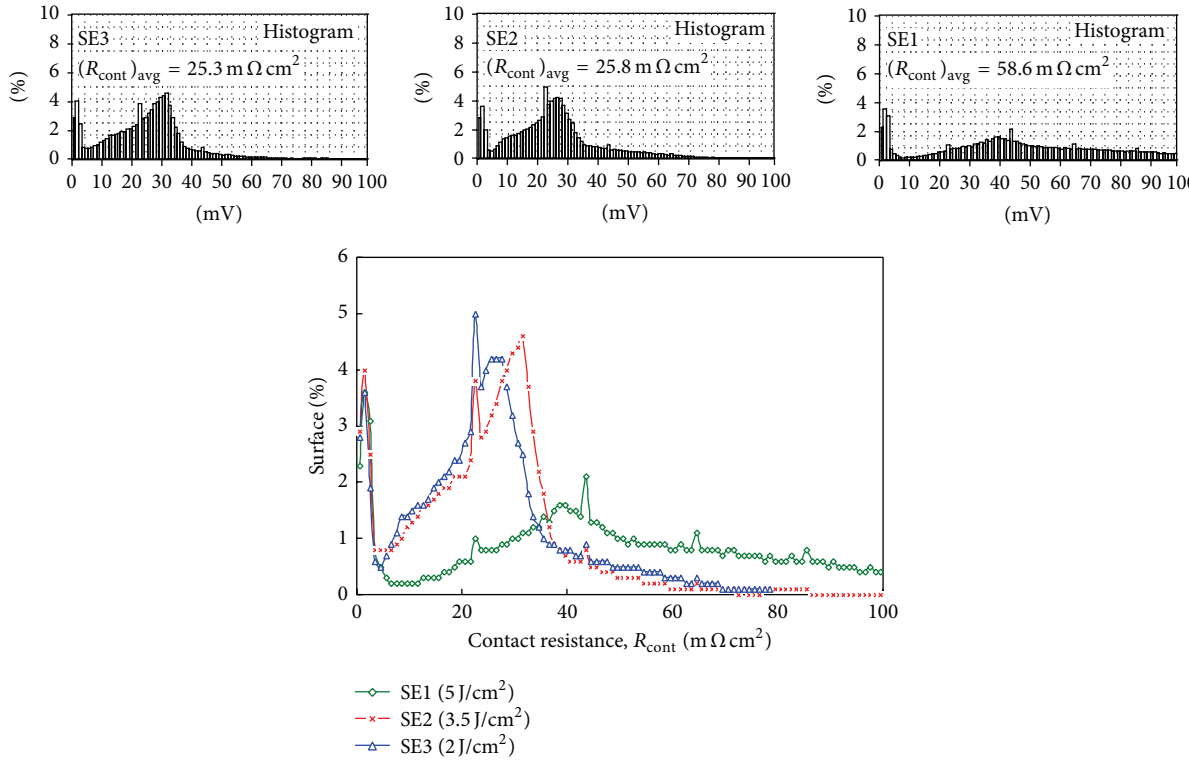

Figure 6: Comparison of distribution profiles of LBIC-contact resistances (in mΩ-cm^2) for SE mc-Si solar cells with different laser fluences. The top inserts are real photos measured for average values of contact resistance, $(R_{cont})_{avg}$, with three developed SE samples.

one can explain that the cell has a higher value of J_{sc} and thus higher conversion efficiency as verified in Figure 4.

Figure 6 shows the comparison of a distribution profile of LBIC for SE mc-Si solar cells with different laser fluences, imaged using a microwave-induced photoconductance decay (μ-PCD) system at the injection level of approximately 10^{16} atoms/cm^3. The average LBIC-contact resistance values (in mΩ-cm^2) are approximately 58.6, 25.8, and 25.3, with laser fluences (in J/cm^2) of 5 (SE1), 3.5 (SE2), and 2 (SE3), respectively. For an LBIC-contact resistance lower than 40.5 mΩ-cm^2 in these distribution profiles, the surface fractions with SE1, SE2, and SE3 demonstrate the values of 37.6%, 86.9%, and 89.6%, respectively. The SE1 cell shows lower surface-fraction value, LBIC, and contact resistance, which is primarily because of the laser-induced defect and increasing minority carrier recombination [19]. The optimal value of the lowest contact resistance with the highest surface fraction (in the case of SE3) also clearly illustrates the optimal solar-cell performance. These results are shown in the insert of Figure 4.

To maximize usage of solar energy for industrial applications, LBIC is used to show the power loss of the developed SE mc-Si solar cells. Figure 7 shows distribution profiles of power loss (mW/cm^2) for the SE mc-Si solar cells with different laser fluences. The average LBIC power loss values are 23.63, 2.62, and 2.33 mW/cm^2, for laser fluences (J/cm^2) of 5 (SE1), 3.5 (SE2), and 2 (SE3), respectively. The fluctuations in the laser fluence can lead to the formation of surface defects in the laser opening regions. The grain boundaries ablated by lasers can cause discontinuities in the opening region and form a shunting pathway. Moreover, there is a local ideality factor greater than unity after subsequent metallization [20]. This shows that there are distinct surface morphologies with the different laser fluences as previously illustrated in Figure 2. Therefore, the optimal SE3 shows the smallest loss of power with the least impact of laser-induced defects in a space charged region. Superior solar-cell performance can be acquired for large-area and high-volume commercial production.

4. Conclusion

The characteristics of the large-area mc-Si solar cells fabricated on SE processes with three different laser opening fluences were evaluated. The optimal efficiency result of 15.95% was achieved by the SE3 cell (2 J/cm^2), which effectively yielded a gain of 0.48%$_{abs}$ compared with that of the Ref. cell. This indicates that, as the lower laser power is applied, fewer defects and discontinuities are produced on the laser-opening region. Despite the efficiency, the SE3 cell has superior features to the other solar cells. It has an average lifetime of 8.082 μs, a short-circuit current density of 34.28 mA/cm^2, an average EQE of 68.6%, a contact resistance of 25.3 mΩ-cm^2, and an average power loss of 2.33 mW/cm^2. All the improvements to performance show fewer losses because of less laser-induced damage to the cell.

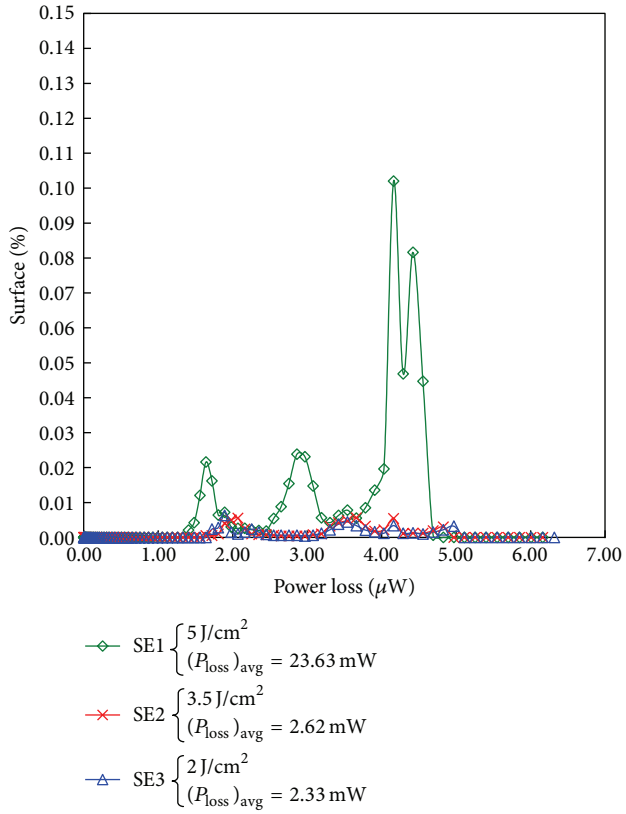

FIGURE 7: Comparison of distribution profile and average value of power loss (in mW/cm^2) for SE mc-Si solar cells with different laser fluences.

The laser opening process has the characteristics of simplicity, reliability, rapidity, and cost effectiveness. These features make SE consistent with high-efficiency mc-Si solar cells. In industrial implementation, great cost reductions to manufacturing SE solar cells are expected, making it viable for industrial applications for the foreseeable future. Improving the mc-Si texturing quality and implementing novel process features will be a focus of future studies; this will include different material coatings to obtain high-efficiency solar cells.

Conflict of Interests

The authors declare that there is no conflict of interests regarding the publication of this paper.

Acknowledgment

This study is supported by the National Science Council of the Republic of China, under Contract nos. NSC 102-2221-E-019-040-MY3 and NSC 101-2221-E-019-043.

References

[1] M. J. Kerr, J. Schmidt, A. Cuevas, and J. H. Bultman, "Surface recombination velocity of phosphorus-diffused silicon solar cell emitters passivated with plasma enhanced chemical vapor deposited silicon nitride and thermal silicon oxide," *Journal of Applied Physics*, vol. 89, no. 7, pp. 3821–3826, 2001.

[2] J. Szlufcik, H. E. Elgamel, M. Ghannam, J. Nijs, and R. Mertens, "Simple integral screenprinting process for selective emitter polycrystalline silicon solar cells," *Applied Physics Letters*, vol. 59, no. 13, pp. 1583–1584, 1991.

[3] R. Barinka, I. Köhler, W. Stockum et al., "Advanced selective emitter solar cell process with use of screen-printable etching paste," in *Proceedings of the 23rd European Photovoltaic Solar Energy Conference and Exhibition (EPVSEC '08)*, pp. 1760–1763, Valencia, Spain, 2008.

[4] U. Jäer, M. Okanovic, M. Hörteis, A. Grohe, and R. Preu, "Selective emitter by laser doping from phosphorsilicate glass," in *Proceedings of the 24th European Photovoltaic Solar Energy Conference (EPVSEC '09)*, pp. 1740–1743, Hamburg, Germany, 2009.

[5] M. Gauthier, M. Grau, O. Nichiporuk, F. Madon, V. Mong-The Yen, and N. Le Quang, "Industrial approaches of selective emitter on multicrystalline silicon solar cells," in *Proceedings of the 24th European Photovoltaic Solar Energy Conference (EPVSEC '09)*, pp. 1875–1878, Hamburg, Germany, 2009.

[6] U. Besi-Vetrella, L. Pirozzi, E. Salza et al., "Large area, screen printed silicon solar cells with selective emitter made by laser overdoping and RTA spin-on glasses," in *Proceedings of the 26th IEEE Photovoltaic Specialists Conference*, pp. 135–138, October 1997.

[7] J.-J. Ho, Y.-T. Cheng, J.-J. Liou et al., "Advanced selective emitter structures by laser opening technique for industrial mc-Si solar cells," *Electronics Letters*, vol. 46, no. 23, pp. 1559–1561, 2010.

[8] J.-J. Ho, Y.-T. Cheng, W. J. Lee et al., "Investigation of low-cost surface processing techniques for large-size multicrystalline silicon solar cells," *International Journal of Photoenergy*, vol. 2010, Article ID 268035, 6 pages, 2010.

[9] Y.-T. Cheng, J.-J. Ho, S.-Y. Tsai et al., "Efficiency improved by acid texturization for multi-crystalline silicon solar cells," *Solar Energy*, vol. 85, no. 1, pp. 87–94, 2011.

[10] J.-Y. Lee and S.-W. Glunz, "Investigation of various surface passivation schemes for silicon solar cells," *Solar Energy Materials and Solar Cells*, vol. 90, no. 1, pp. 82–92, 2006.

[11] J. P. McDonald, V. R. Mistry, K. E. Ray, S. M. Yalisove, J. A. Nees, and N. R. Moody, "Femtosecond-laser-induced delamination and blister formation in thermal oxide films on silicon (100)," *Applied Physics Letters*, vol. 88, no. 15, Article ID 153121, 2006.

[12] V. Juzumas, A. Galdikas, A. Melninkaitis, and G. Slekys, "Laser ablation passivation barrier layer coated silicon using high repetition rate femtosecond pulses for selective emitter formation," in *Proceedings of the 23rd European Photovoltaic Solar Energy Conference and Exhibition (EPVSEC '08)*, pp. 1397–1401, Valencia, Spain, 2008.

[13] U.S. Department of Energy, "National solar technology roadmap: wafer-Silicon PV," Tech. Rep. NREL/MP-520-41733, June 2007.

[14] E. Lohmuller, B. Thaidigsmann, M. Pospischil et al., "20% Efficient passivated large-area metal wrap through solar cells on boron-doped Cz silicon," *IEEE Electron Device Letters*, vol. 32, no. 12, pp. 1719–1721, 2011.

[15] H. Boubekeur and M. Boumaour, "Impact of lateral junction on selective emitter solar cell performance," *Solar Energy Materials and Solar Cells*, vol. 56, no. 1, pp. 7–15, 1998.

[16] S. Hopman, A. Fell, K. Mayer et al., "Study on laser parameters for Silicon solar cells with LCP selective emitters," in *Proceedings of the 24th European PV Solar Energy Conference and Exhibition*, pp. 1–5, Hamburg, Germany, 2009.

[17] C.-H. Lin, S.-P. Hsu, J.-J. Liou, C.-P. Chuang, W.-H. Lu, and W.-L. Chang, "Characterization of selective-emitter solar cells consists of laser opened window and subsequently screen-printed electrodes," in *Proceedings of the 35th IEEE Photovoltaic Specialists Conference (PVSC '10)*, pp. 3523–3526, Honolulu, Hawaii, USA, June 2010.

[18] M. Abbott, P. Cousins, F. Chen, and J. Cotter, "Laser-induced defects in crystalline silicon solar cells," in *Proceedings of the 31st IEEE Photovoltaic Specialists Conference*, pp. 1241–1244, Boca Raton, Fla, USA, January 2005.

[19] P. Engelhart, S. Hermann, T. Neubert et al., "Laser ablation of SiO_2 for locally contacted Si solar cells with ultra-short pulses," *Progress in Photovoltaics: Research and Applications*, vol. 15, no. 6, pp. 521–527, 2007.

[20] M. D. Abbott, J. E. Cotter, F. W. Chen, T. Trupke, R. A. Bardos, and K. C. Fisher, "Application of photoluminescence characterization to the development and manufacturing of high-efficiency silicon solar cells," *Journal of Applied Physics*, vol. 100, no. 11, Article ID 114514, 2006.